Stabilization of the Biologically Active Conformation of the Principal Neutralizing Determinant of HIV-1_{IIIB} Containing a *cis*-Proline Surrogate: ^{1}H NMR and Molecular Modeling Study†

Julian Garcia,*,‡ Pascal Dumy,*,‡ Osnat Rosen,§ and Jacob Anglister§

LEDSS, University Joseph Fourier of Grenoble, BP 53, 38041 Grenoble Cedex 9, France, and Department of Structural Biology, Weizmann Institute of Science, Rehovot 76100, Israel

Received December 22, 2005; Revised Manuscript Received February 10, 2006

ABSTRACT: The V3 loop is part of the gp120 glycoprotein, an extracellular protein located on the membrane of the human immunodeficiency virus (HIV-1). This loop is significantly important in many biological processes of the virus and contains the principal neutralizing determinant (PND). The PND is one of the most variable regions of the envelope, and this is probably related to the ability of the HIV virus to escape the immunologic defenses of the target host. Particular attention has been paid to the central part of the V3 loop which contains a highly conserved GPGR/GPGQ sequence and represents the binding site for antibodies. Many attempts have been made to design synthetic peptides as mimics of the V3 loop capable of eliciting immune response. However, this strategy suffers from the great conformational flexibility small peptides have in solution, which together with bioavailability represents the most important limitation to the usefulness of synthetic peptides as drugs and as synthetic immunogens. The use of conformationally constrained peptides can alleviate this problem. Early works using NMR studies have shown that a $V3_{IIIB}$ loop-derived peptide is conformationally heterogeneous when free in water. Upon complexation with 0.5β, a monoclonal neutralizing antibody specific for the HIV-1_{IIIB} strain, it adopts a β-hairpin conformation with the central proline forming a type VIb β-turn. In this study, we report the design and characterization of a conformationally restricted peptide with a sequence identical to that previously described, but with thiazolidine derivatives replacing the proline. The affinity of the 2,2-dimethylthiazolidine derivative for 0.5β demonstrates that this moiety can successfully be used to mimic the proline in a cis conformation. This peptide not only displays a high propensity to adopt a β-hairpin conformation but also retains the type VIb RGPG β-turn similar to that found in the native complex. These compounds could help in elaborating more efficient immunogens for HIV-1 synthetic vaccine development.

Development of acquired immunodeficiency syndrome (AIDS) in humans results from the destruction of macrophages and T lymphocyte cells by HIV virus type 1 (HIV-1)[1] (*1*). An early event of infection involves specific binding of HIV particles to the immunoglobulin-like domains of the CD4 antigen receptor, a protein which is expressed by these cells and normally functions in immune recognition. This interaction proved to be sufficient for binding to the cell but not for cellular fusion to occur. It also appeared that in addition to CD4 a chemokine receptor, usually CCR5 or CXCR4, was required for the virus to enter the target cell (*2*−*6*).

Entry of HIV into the host cells is a multistep process mediated essentially by viral envelope glycoproteins, which are extensively glycosylated and displayed at the surface of the virus. These proteins are trimeric oligomers organized within two subunits, a surface-exposed part constituted by the gp120 glycoprotein and a transmembrane part, the gp41 glycoprotein, associated together by noncovalent interactions. The gp120 glycoprotein consists of five hypervariable loops designated V1−V5 (*7*), four of which (V1−V4) are linked at their bases by disulfide bonds (*8*). It is now well established that among these, the V3 loop is of crucial importance. First, this loop is directly involved in the interaction of the virus with both CD4 and the chemokine receptors (*9*, *10*). Interaction between the gp120−CD4 complex and the coreceptor is not possible when the V3 loop is blocked by an antibody (*9*). Furthermore, the V3 loop is the most critical determinant for cellular tropism despite the sequence variations (*11*, *12*). This result is supported by the fact that mutation of just one amino acid is sufficient to

† This study was supported by the NIH Grant GM53329 (J.A.), The Institut Universitaire de France (P.D.), and ACI Grant 02L0525 (P.D.).

* To whom correspondence should be addressed. E-mail: julian.garcia@ujf-grenoble.fr. Phone: ++33 (0)4 76 51 44 34. Fax: ++33 (0)4 76 51 43 82.

‡ University Joseph Fourier of Grenoble.

§ Weizmann Institute of Science.

[1] Abbreviations: HIV-1, human immunodeficiency virus-1; PND, principal neutralizing determinant; ELISA, enzyme-linked immunosorbent assay; DQF-COSY, double-quantum-filtered correlation spectroscopy; MD, molecular dynamics; NMR, nuclear magnetic resonance; NOESY, nuclear Overhauser enhancement spectroscopy; pH*, uncorrected pH-meter reading; E-COSY, exclusive correlation spectroscopy; TOCSY, total correlation spectroscopy; ROESY, rotating frame Overhauser enhancement; 2D, two-dimensional; rmsd, root-mean-square deviation.

10.1021/bi052615k CCC: $33.50
Published on Web 03/09/2006

render the host cell infected. Finally, and most interestingly the principal neutralization determinant (PND) of HIV-1 has been mapped to the V3 loop (*13*).

Many synthetic peptides have been based on a PND-like structure to generate immune responses and elicit antibodies capable of neutralizing HIV-1 (*14*−*17*). However, the extreme amino acid sequence variability within the V3 loop has hampered attempts to construct immunogens capable of inducing broadly reactive neutralizing anti-HIV antibody responses. Nevertheless, LaRosa et al. have shown in an early work performed on 245 different HIV-1 isolates that although certain amino acids are highly variable in their position, others are well-conserved (*18*). This was particularly true for the Gly-Pro-Gly tripeptide located near the crest of the loop and present in ~90% of the sequences. One strategy to overcome the problem of sequence variability in HIV vaccine design is to use a large panel of multicomponent immunogens corresponding to a definite epitope, yet it is not clear whether this approach should be based principally on the composition of the amino acid sequence, the higher-order structure of the viral proteins, or a combination of the two.

Numerous structure determinations have been conducted upon a variety of V3 loop-derived peptides, the aim of these studies being to determine common structural features that could provide pharmacophore fingerprints. These peptides were shown to have low propensity to form secondary structures and were conformationally averaged when free in solution, often differing from the structures their cognate sequences adapt in the native protein (*16*, *20*, *21*). X-ray crystal structures of the V3 loop in interaction with Fab fragments of antibodies raised against V3 peptides have been reported (*20*, *22*−*24*). Liquid (*25*−*28*) and solid state (*29*, *30*) NMR studies have also been conducted on complexes of V3 peptides with Fab and Fv fragments of an anti-gp120 antibody. These studies focused mainly on the highly conserved Gly-Pro-Gly-Arg motif which is a part of or is very close to the epitope of many antibodies raised against HIV-1 (*13*, *18*, *20*). They revealed an overall conformation consisting of a β-hairpin with a central type I, a type II, and a complex double β-turn in the region of the Gly-Pro-Gly-Arg motif for HIV-1_{MN} V3 peptides and a type VI β-turn for HIV-1_{IIIB} V3 peptides. They also pointed out that the V3 loop adopts an antibody-dependent conformation when bound to the antibody while it is conformationally heterogeneous in the unbound state.

To overcome the great conformational flexibility of V3 loop segments in aqueous solution, numerous attempts have been made to stabilize the secondary structure mimicking the native structure, which is potentially the most immunogenically interesting state. These attempts included chemical modification of amino acids (*15*, *20*), addition of trifluoroethanol (*31*−*33*), cyclization of the peptide (*31*, *32*, *34*), glycosylation (*35*, *36*), and conjugation with BPTI protein (*21*).

Pseudoproline (ΨPro) has previously been used to stabilize the Xaa−Pro peptide bond in the cis conformation. In particular, the propensity of pseudoproline to form a trans or cis peptide bond was shown on di- and tripeptides to depend on the degree of substitution at position C2 (*37*, *38*). 2,2-Dimethylthiazolidine was introduced into a cyclic V3 peptide (*39*) to mimic the proline cis conformation, which was proposed to be the biologically active form of $V3_{IIIB}$ peptides (*27*, *40*, *41*). However, NMR data indicated that this peptide was conformationally heterogeneous since it existed in a mixture of three different conformers in DMSO, the major form being attributed to a cis amide bond. Furthermore, the V3 fragment considered was based on a $V3_{MN}$ strain which was previously described to form a type II β-turn with a *trans*-proline peptide bond (*20*), and with amino acid sequence well different from that of the $V3_{IIIB}$ strain, particularly in the relevant GPGR central part. Even though this peptide was able to elicit a specific immune response, no attempt was made to demonstrate that it could be recognized by anti-HIV antibodies.

Most HIV-1 neutralizing antibodies are directed against the V3 loop. One of these, namely, 0.5β, is a potent specific antibody that has been raised against the gp120 HIV-1_{IIIB} strain (*42*). It was previously shown that this antibody binds to P1053, an 18-residue peptide, with almost the same affinity as RP135, a six-amino acid longer sequence mapped as the principal neutralizing determinant (*42*).

In this paper, we present an NMR and molecular modeling study of $V3_{IIIB}$ peptides, analogous to that described by Anglister and co-workers (*27*), thus allowing direct comparison with the relevant biological form. We also evaluate the effect of substitution on the C2 position of thiazolidine. Three 18-residue peptides were synthesized with proline in the middle of the sequence (P1035), and with thiazolidine (Pdht) or 2,2-dimethylthiazolidine (Pdmt) replacing the native proline.

We present conclusive evidence that the 2,2-dimethylthiazolidine containing peptide in pure water can successfully mimic a type VI *cis*-proline turn and can bind the 0.5β antibody.

MATERIALS AND METHODS

Peptide Synthesis. Peptides were synthesized by standard solid-phase peptide synthesis (SPPS) methods (*43*, *44*), as previously described (*45*). The Fmoc (N9-fluorenylmethoxycarbonyl)/*t*Bu (*tert*-butyl) chemistry was used on Wang resin (*46*). Briefly, the two pseudoprolines were first prepared from the cysteine-derived amino acid and introduced during SPPS as preformed dipeptide building blocks [Fmoc-Gly-Cys($\psi^{H,H}$-pro)-OH and Fmoc-Gly-Cys($\psi^{Me,Me}$pro)-OH for Pdht and Pdmt, respectively]. After cleavage from the resin and deprotection, the linear peptides were precipitated in diethyl ether, filtered, and purified by RP-C18 HPLC using a gradient of acetonitrile and water each containing 0.09% trifluoroacetic acid (TFA). The synthesis afforded pure (≈70% yield) peptides as judge by ES-MS (electrospray mass spectrometry) and NMR spectroscopy. Pdht: ES-MS *m*/*z* 2029.7 ($[M + H]^+$), 1015.5 ($[M + 2H]^{2+}/2$). Pdmt: ES-MS *m*/*z* 2057.8 ($[M + H]^+$), 1029.6 ($[M + 2H]^{2+}/2$).

NMR Spectroscopy. NMR spectra were obtained at 800 and 500 MHz with Varian Inova and Bruker Avance spectrometers, respectively. Peptide samples were dissolved in a mixture of 95% H_2O and 5% ^2H_2O or 99.9% ^2H_2O to a final concentration of 2−3 mM at 15 °C. The pH* was adjusted to 5.7 for all measurements. A set of two-dimensional (2D) spectra, including TOCSY (*47*), DQF-COSY (*48*), E-COSY (*49*), ROESY (*50*), and NOESY (*51*) spectra, were acquired with a 1.5 s steady-state recovery time and mixing times (t_m) of 60 ms for TOCSY and 80, 110,

and 250 ms for NOESY. Water suppression was achieved by appending an excitation-sculpting module (*52*) to the nonselective detection pulse and with selective Gaussian-shaped pulses of 3−5 ms. All spectra were acquired in phase sensitive mode using TPPI (*53*), the States method (*54*), or gradient-assisted coherence selection (echo−antiecho) (*55*). The spin-lock mixing of the TOCSY experiment was obtained with MLEV17 (*56*) or DIPSI-2 (*57*) pulse trains when $\gamma B_2/2\pi = 9-10$ kHz. The acquisitions were performed over a spectral width of 10 ppm in both dimensions, with a matrix size of 2048−4096 data points in t_2 and 256−512 points in t_1, and 32−128 scans/t_1. All spectra were referenced with external TSP-d_4. Data processing and analysis were performed using Felix (version 2001, Accelrys, San Diego, CA) with shifted (60−90°) square sine-bell apodization and polynomial baseline correction for NOESY data.

Dihedral Angles Restraints. $^3J_{NH-H\alpha}$ coupling constants were mostly extracted from the high-resolution one-dimensional spectrum run at 800 MHz or from a high-resolution DQF-COSY experiment in case of dramatic overlapping. The $^3J_{NH-H\alpha}$ coupling is a function of the dihedral angle ϕ, as given by the modified Karplus equation (*58*) where $^3J_{NH-H\alpha} = 6.51 \cos^2(\phi - 60) - 1.76 \cos(\phi - 60) + 1.60$. The coupling constants were derived from the amide splitting in the one-dimensional spectra or from cross-peaks in DQF-COSY spectra and were transformed to ϕ values. Twelve backbone dihedral angles were introduced as restraints, allowing a range of ±20° on the calculated values. Stereospecific assignments for β-methylene protons were achieved by combining qualitative analysis of $^3J_{H\alpha-H\beta}$ coupling constants extracted from an E-COSY spectrum, and interproton HN−Hα distances determined from ROESY spectrum. A value around −60°, 60°, or 180° ± 20° was subsequently attributed to seven dihedral angles (χ_1). Force constants in the range of 30−50 kcal mol^{-1} rad^{-2} were applied.

Distance Restraints. For Pdmt, interproton distance restraints were derived from cross-peaks in NOESY spectra recorded with mixing times of 80, 110, and 250 ms. The cross-peaks were analyzed and integrated using the integration routine in Felix (version 2001, Accelrys). Approximate interproton distance restraints were calculated using the isolated two-spin approximation relationship $r_{ij} = r_{kl}(\sigma_{kl}/\sigma_{ij})^{1/6}$, where σ_{ij} and σ_{kl} are the NOE intensities for the atom pair i and j and atom pair k and l separated by distances r_{ij} and r_{kl}, respectively. The βH1 and βH2 protons of the pseudoproline are nondegenerate, and their internuclear distance is invariant with the peptide conformation. Therefore, this internuclear distance, whose value is 1.79 Å, was taken as a reference distance. When necessary, methyl and methylene groups were replaced with pseudoatoms, which were used as reference points for the experimental distance constraints. The distances involving such pseudoatoms were corrected according to the rules formulated by Wüthrich (*59*). The distances were used as restraints, using force constants that ranged from 20 to 50 kcal mol^{-1} Å^{-2} and a ±10% range put on the calculated distances, to represent the upper and lower bounds. The total number of distance restraints was 137.

Interproton distances thus calculated were refined by the iterative relaxation matrix approach (IRMA) (*60*). This is a computational method based on NMR relaxation theory (*61*). Structure calculations were performed on a Silicon Graphics O2 irix 6.5 workstation using the NMRchitect and InsightII/Discover (Version 2000, Accelrys) modules within the Accelrys software package. For a given molecular structure, the NOE intensities were calculated by the IRMA which takes into consideration molecular flexibility and spin diffusion by numerically solving for the entire spin-relaxation network, thus providing more accurate distance restraints than the isolated two-spin approximation. The calculated NOE intensities and experimental NOE intensities were compared, and the structure was gradually refined during an iterative process, until good matching between the two was as close as possible. As part of each IRMA cycle, a protocol including restrained molecular dynamics (rMD) and restrained energy minimization (rEM), was carried out to minimize the structure based on the refined distance and torsion angle restraints. After minimization, a new IRMA calculation was executed, and distance constraints were updated. To measure the quality of IRMA-calculated structure obtained in each cycle, a series of *R*-factors which compare experimental data and model structures were calculated (*62*). In this paper, we present the results obtained for one of the most important *R*-factor, the crystallographic-like factor defined by $R = \sum|I_c - I_e|/\sum|I_e|$, where I_c and I_e denote the calculated and experimental NOE intensities, respectively. The *R*-factors and rms differences in the atom coordinates between the structures were the two criteria used to monitor the convergence. The process was carried through to convergence. Assuming isotropic motion, a single rotational correlation time (τ_c) of 2.0 ns was used for the whole molecule. This value was estimated by measuring the initial NOE buildup rate for the reference peak.

Two structures of the peptide were used as the starting conformation for the simulations as stated below. The first structure was built in a fully extended conformation with the Biopolymer module in InsightII and noted Init-A. The second structure noted Init-B was generated from that obtained by Anglister and co-workers (*27*; PDB entry 1B03), after replacement of the proline residue with a 2,2-dimethylthiazolidine moiety.

Structure Calculations. To more widely explore conformational space, we used a high-temperature simulated annealing protocol for rMD simulations. Calculations were performed in vacuo, and the energy of the system was calculated by the consistent CVFF force field (version 2.3). The NOE and dihedral restraining functions used were standard square-well effective potentials, and to shorten the range of Coulomb interaction, a distance-dependent relative dielectric constant, ϵ_r, was used ($\epsilon_r = 4r$). To prevent the ω-torsions from flipping to the cis conformation during the simulations, a force constant of 100 kcal mol^{-1} rad^{-2} was applied for all, but preceding ΨPro bond.

In the simulations, starting structures were subjected to the following protocol with appropriate restraint weights which were modulated by multiplying the force constants with a scaling factor. The starting structures were first subjected to 500 cycles of rEM with conjugate gradients. The initial velocities were assigned with a Maxwell distribution at 600 K. The system was gradually heated from 0 to 600 K during the first 2 ps and then maintained at 600 K for the next 40 ps. The step size of the integrator was set to 1 fs. During this phase of the simulation, force constants

were gradually increased by a factor of 2 in the first 10 ps and then held constant at this level during the high-temperature phase. The system was slowly cooled to 300 K, in steps of 100 K, for 30 ps and then maintained at 300 K for an additional 20 ps. During the cooling and equilibrium phases, distance and dihedral angle force constants were gradually decreased to their initial value. The last 10 coordinate sets were averaged and subjected to a final 1000 steps of restrained energy minimization to generate the restrained structures.

To improve the quality of the NOE restraint set, the theoretical NOESY spectrum was back-calculated using the matrix doubling module of Felix and compared with the experimental one. This module calculates the dipole−dipole relaxation matrix for a system of protons and converts them into a NOESY spectrum. The back-calculated 2D NOE spectra were compared with the experimental (80, 110, and 250 ms) 2D NOE spectra to determine how well the model structure fits the experimental data. Since NOE signals are proportional to r^{-6}, a small error in the distance between two protons can lead to a large change in the intensity of the cross-peak for these two protons. A deviation of a factor of 2.5 (±15% experimental error in distance) between the volumes of the calculated cross-peaks and the experimental values was considered to be a violation. To minimize the differences between calculated and experimental NOESY spectra, the distances corresponding to these violations were progressively adjusted to the experimental values through further refinement of the corresponding new sets of NOE restraints, and a new MD was performed until good concordance was reached between theoretical and experimental NOESY spectra.

Binding Essay Competitive ELISA. Microtiter plates with 96 wells (Maxi Immunosorp plates by Nunc) were coated with each of the peptides (1 μg/mL) in 0.05 M bicarbonate buffer (pH 9.6) for 20 h at 37 °C. The wells were washed twice with phosphate-buffered saline (PBS) containing 0.5% Tween 20 (washing buffer), following by blocking with PBS containing 2% newborn calf serum for 45 min at 37 °C. Samples containing 0.8 μg/mL 0.5β antibody were separately incubated with different dilutions of each peptide for 30 min at room temperature (RT). The antibody:peptide dilutions range from 3:1 to 1:72900 (0.08−1560 μg/mL). One hundred microliters of each mixture was then added to the wells and incubated for 30 min at RT, followed by four steps of washing with the washing buffer. Secondary antibody (goat anti-mouse conjugated peroxidase, Jackson ImmunoResearch Laboratories Inc.) was added for 30 min at RT. In the final step, the plate was washed four times and developer (0.028 M citric acid, 0.044 M Na_2HPO_4, 1 mg/mL ABTS, and 0.003% H_2O_2) was added. The absorbance value was read at 620 nm by a SPECTRAFluor Plus machine. Affinity constants were estimated by the peptide concentration at 50% absorbance.

RESULTS

NMR studies were performed on three peptides, designated P1053, Pdht, and Pdmt. All these sequences are identical (RKSIRIQRGPGRAFVTIG) except for the replacement of the proline in position 10 with a thiazolidine for Pdht and with a 2,2-dimethylthiazolidine for Pdmt (Figure 1). Structural features of the P1053 sequence when bound to a neutralizing antibody have been previously reported by the Anglister group (*27*). The solution conformation of the native peptide free in solution was described by the same group but for a longer sequence, denoted RP135-GKK (*33*).

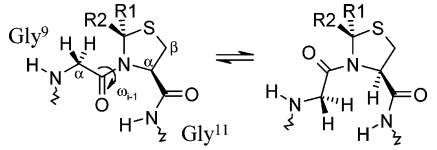

FIGURE 1: Model of the Gly^9-Xaa^{10}-Gly^{11} structure in trans and cis conformations, depending upon the ω_{i-1} value. Xaa represents either thiazolidine denoted Dht (R1 = R2 = H) or 2,2-dimethylthiazolidine denoted Dmt (R1 = R2 = CH_3).

Table 1: Proton Chemical Shift Assignments for the Pdmt Sequence[a]

residue	HN	Hα	Hβ	Hγ	others
Arg^1	na[b]	4.13	1.91	1.67	$CH_2\delta$ 3.22
Lys^2	na[b]	4.52	1.83	1.45	$CH_2\delta$ 1.71; $CH_2\epsilon$ 2.99
Ser^3	8.60	4.64	3.82		
Ile^4	8.41	4.39	1.85	1.47, 1.18	$CH_3\gamma$ 0.90; $CH_3\delta$ 0.86
Arg^5	8.52	4.63	1.86, 1.73	1.61	$CH_2\delta$ 3.14
Ile^6	8.48	4.41	1.81	1.48, 1.17	$CH_3\gamma$ 0.91; $CH_3\delta$ 0.85
Gln^7	8.71	4.53	2.05, 1.92	2.26	$NH_2\delta$ 7.55, 6.92
Arg^8	8.59	4.58	1.87, 1.75	1.64	$CH_2\delta$ 3.19
Gly^9	8.34	4.21, 3.88			
Dmt^{10}		5.10	3.56, 3.32		$CH_3\delta$ 1.79, 1.87
Gly^{11}	8.71	4.11			
Arg^{12}	8.33	4.44	1.88, 1.71	1.60	$CH_2\delta$ 3.18
Ala^{13}	8.18	4.42	1.32		
Phe^{14}	8.28	4.89	3.10, 3.00		Hδ 7.20; Hϵ 7.33; Hη 7.29
Val^{15}	8.34	4.40	2.04	0.92	
Thr^{16}	8.44	4.64	4.15	1.19	
Ile^{17}	8.50	4.25	1.90	1.47, 1.19	$CH_3\gamma$ 0.93; $CH_3\delta$ 0.85
Gly^{18}	8.18	3.81			

[a] Proton assignments are in H_2O at 15 °C and pH 5.7 (at 800 MHz). [b] Not assigned.

^{1}H NMR Resonance Assignments. All NMR spectra for the three peptides (P1053, Pdht, and Pdmt) were collected with the same conditions of temperature and pH, at 500 and 800 MHz. Individual spin systems were assigned on the basis of an analysis of through-space nuclear Overhauser effect (NOESY and ROESY) and through-bond correlated (DQF-COSY and TOCSY) spectra using well-established sequential strategy methods (*63*). The assigned resonances are given in Table 1 for Pdmt and in the Supporting Information (Tables 2 and 3 for Pdht and P1053, respectively).

Secondary Structure. The propensity to form a β-turn in the GPGR region was evident in the three peptides from NOESY spectra.

P1053 displayed weak $d_{\alpha N}(i, i + 2)$ NOE correlations between Pro^{10} and Arg^{12} typical of β-turns (Figure 2). Further examination of the NOESY spectra revealed strong cross-peaks between Hα of Gly^9 and the Hδ protons of Pro^{10}, indicating that the proline-preceding bond was in the trans configuration (Figure 2). Evidence for some cis conformation was not detected, suggesting that the trans conformation dominated for this peptide. Furthermore, this peptide gave rise to strong $d_{\alpha N}(i, i + 1)$ NOE between Pro^{10} and Gly^{11}, indicative of a reverse type II β-turn. In addition, a weak NOE appeared between the amide proton of Gly^{11} and the Hδ protons of Pro^{10}, indicating a small population of the

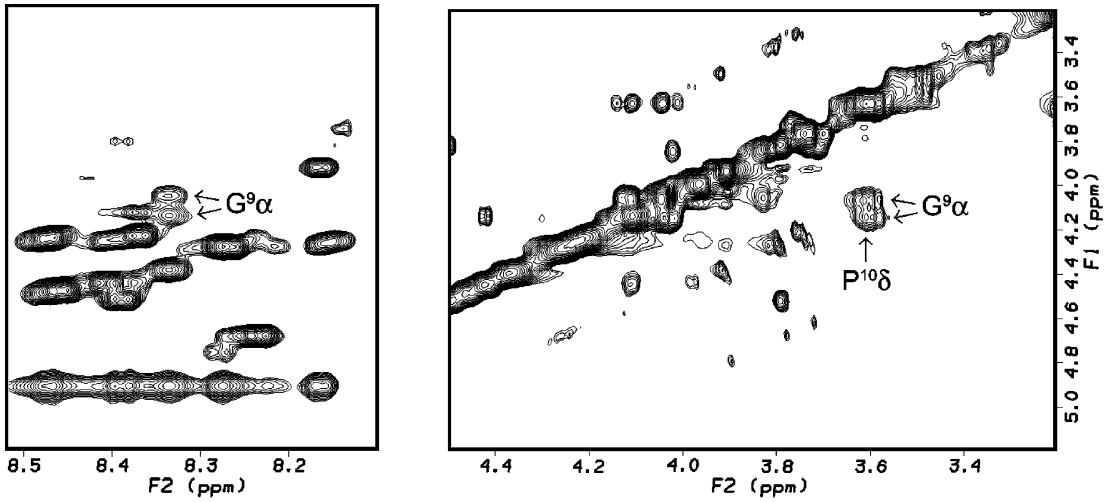

FIGURE 2: Expanded regions of a NOESY spectrum (500 MHz) of P1053 in a 95% H_2O/5% ^2H_2O mixture. Relevant peaks are labeled: NH−Hα region (left) and Hα−Hα region (right).

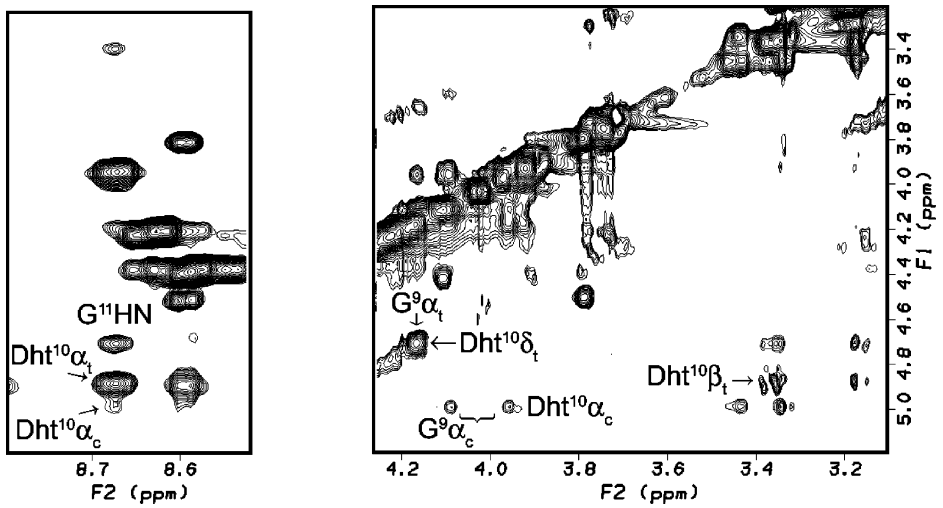

FIGURE 3: Expanded region of the NOESY spectrum (500 MHz) of Pdht in a 95% H_2O/5% ^2H_2O mixture. Relevant peaks are labeled: NH−Hα region (left) and Hα−Hα region (right).

peptide in a type I β-turn. A similar result was also observed for the RP135-GKK peptide (*33*). Although $d_{NN}(i, i + 1)$ NOEs were seen in the NOESY spectra of this peptide, there was no evidence for $d_{\alpha\times e2\beta}(i, i + 3)$, $d_{\alpha N}(i, i + 3)$, or $d_{\alpha N}(i, i + 4)$ NOEs, which ruled out the presence of an ordered α-helix as observed for longer sequences or other V3-derived peptides (*18*).

Besides NOE cross-peaks characteristic of a β-turn in the GPGR crest, the NOESY spectra of Pdht displayed two sets of connectivities for Gly^9 and Dht^{10}, indicating two different conformations in slow exchange on the chemical shift time scale. These two conformers arose from cis−trans isomerization of the Gly^9−Dht^{10} peptide bond. As shown in Figure 3, the major conformer exhibited a strong $d_{N\delta}(i, i + 1)$ NOE between Gly^9 and Dht^{10} and a strong $d_{\alpha N}(i, i + 1)$ NOE between Hα of Dht^{10} and the amide proton of Gly^{11}. This specific combination of NOEs is diagnostic of a type II β-turn with the Gly^9−Dht^{10} peptide bond in the trans conformation. Additionally, weak cross-peaks between the Hα proton of Dht^{10} and the Hα protons of the preceding residue (Gly^9) were detected in the NOESY spectra. Theses correlations are the signature of a minor component having a cis peptide bond (Figure 3). The percentage of the cis conformation was found to be ~20%, on the basis of the intensities of the cross-peaks of the minor and major conformations in the TOCSY spectrum.

As depicted in Figure 4, NOESY spectra of Pdmt gave rise to strong NOEs between Hα protons of Gly^9 and the Hα proton of Dmt^{10}, indicating the presence of a cis peptide bond. No minor conformer due to cis−trans isomerization was detected in all the NMR spectra, indicating that this peptide solely exists in a cis configuration form in water.

The tendency in chemical shifts provides a useful qualitative measure of the presence of secondary structure in peptides and proteins (*64*). Chemical shift indices (CSIs) for the backbone α-protons were calculated using measured chemical shifts and published chemical shifts when the peptide is in a random coil structure. CSI values for the three peptides (P1053, Pdht, and Pdmt) and for RP135-GKK are depicted in Figure 5. A positive deviation from the random coil chemical shift indicates the presence of a β-sheet structure, while a negative deviation for a stretch of at least three or four residues suggests that helical or turnlike structures prevail. CSIs for P1053, Pdht, and RP135-GKK

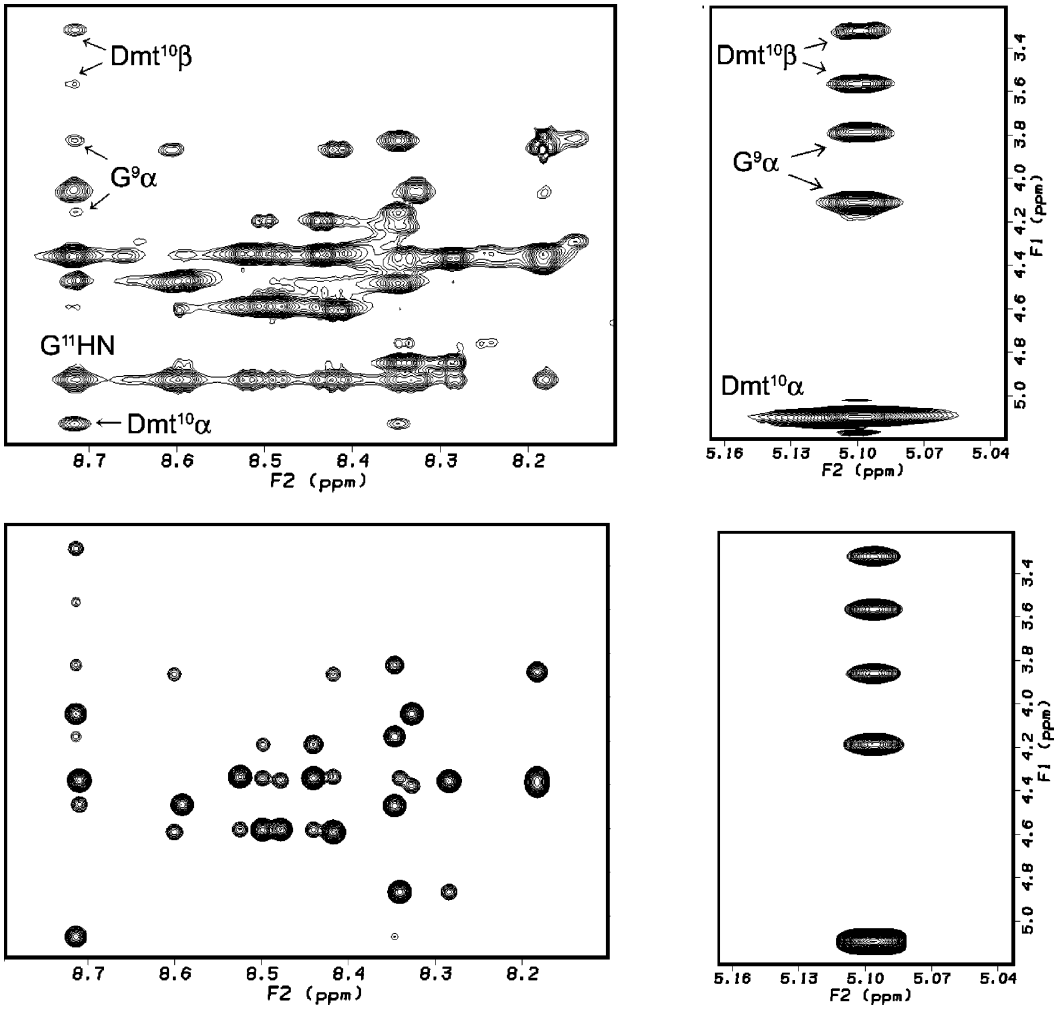

FIGURE 4: Expanded region of the NOESY spectrum (800 MHz) of Pdmt in a 95% H_2O/5% ^2H_2O mixture: (top) fingerprint NH−Hα region and (bottom) corresponding back-calculated NOESY spectrum. Relevant peaks are labeled.

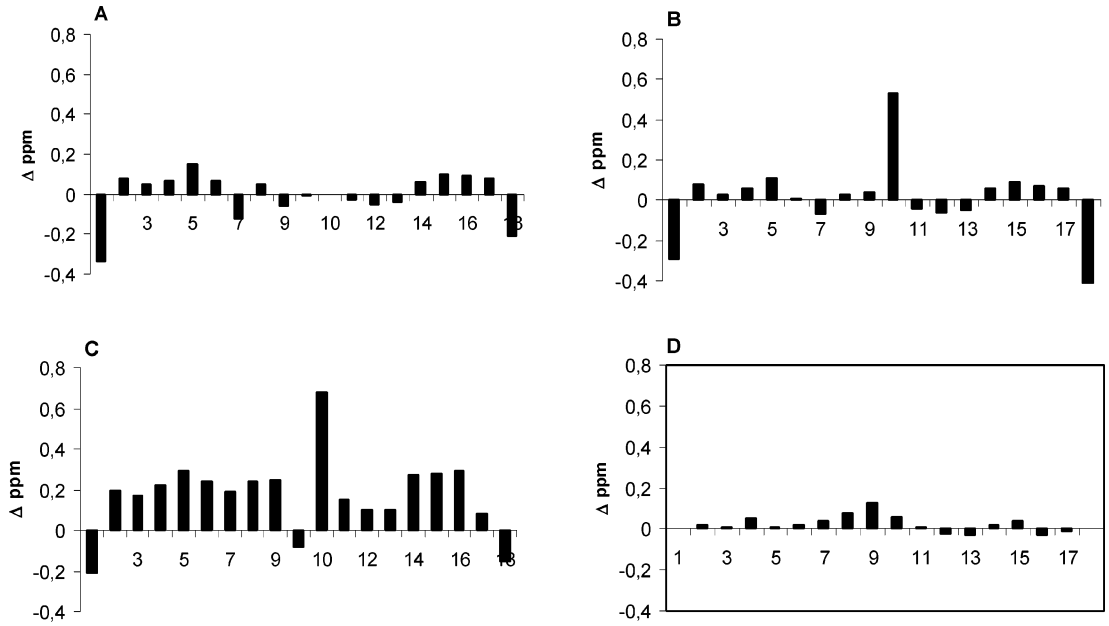

FIGURE 5: Chemical shift index maps for P1053 (A), Pdht (B), Pdmt (C), and RP135-GKK (D) (*33*). Bars above the origin are Hα peaks which resonate downfield of random coil values, and bars below the origin are those which resonate upfield of these values.

are similar (Figure 5A,B,D). They display an irregular pattern of alternating positive and negative CSI values closely approaching typical random coil values. These data show that these peptides are not structured in water. A similar

FIGURE 6: Backbone superimposition of the 10 refined structures. The Dmt^{10} residue is highlighted in gray.

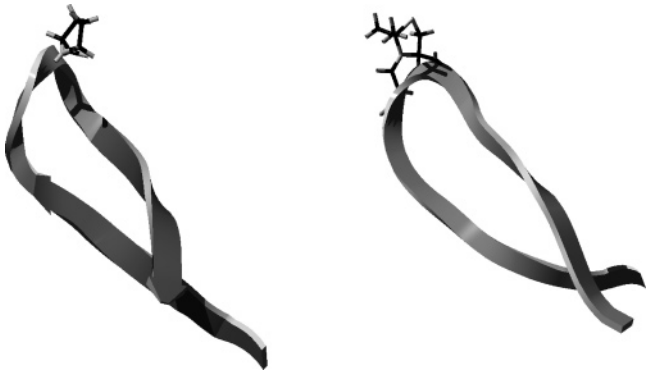

FIGURE 7: Ribbon representation of the backbone of P1053 (left) when bound to the antibody (from PDB entry 1QNZ) and Pdmt free in water (right). This figure was prepared with Swiss-PdbViewer (version 3.7) and POV-Ray (version 3.6).

conclusion was reached by Anglister and co-workers for the RP135-GKK peptide free in solution, which was found to sample a random set of conformations (*33*).

In contrast, a large proportion of the residues of Pdmt have shifts that differ from the random coil values by more than 0.1 ppm, suggesting that Pdmt has a well-defined structure. The positive deviation is indicative of an extended conformation. This result was further supported by the observation of *J* coupling constants in the range of 7−11 Hz (data not shown).

More insight into the secondary structure features of the Pdmt peptide can be gained from a restrained molecular dynamics study with NOE and torsion angle constraints.

Structural Calculations. A model of the solution structure of Pdmt was obtained using hybrid matrix relaxation−simulated annealing calculations, including experimental interproton distance restraints and dihedral angle restraints. The calculations were carried out from two starting structures to ensure that the same final structure was obtained via an approach from different starting directions. One is a fully extended conformation built using InsightII (Init-A), and the other was generated from the structure published by Anglister and co-workers (Init-B) (*27*; PDB entry 1QNZ), which corresponds to the β-hairpin structure that the peptide adopts when bound to a neutralizing antibody (rms difference of 12 Å). The simulated annealing protocol was first performed on both Init-A and Init-B starting structures with initial restraints. The resulting structures were independently submitted to an IRMA for refinement. Over the course of six IRMA iterations, convergence of structure was indicated by the leveling off of *R*-factors, which meant a good fit between the final structure and the experimental data. For the sixth refinement, the structure was taken five separate times through the simulated annealing protocol with randomized velocity seeds. A total of 10 refined structures were obtained, five from each set of starting structures.

Good convergence was achieved for these structures, which had a pairwise rmsd ranging from 0.54 to 0.93 Å. For small peptides, *R*-factors in the range of 0.30−0.50 have been reported (*62*). This is considered a reasonably good value in view of the sparse NMR data generally observed for these molecules. Furthermore, the great majority of distances satisfied the restraints fairly well, with no violation greater than 0.2 Å being observed for these structures. Superposition of the various structures displayed in Figure 6 showed good homogeneity of the structures generated by rMD simulation and indicated that a similar conformation could be approached from very different regions of conformational space. The atomic rmsd values for the starting models and for the restrained structures are displayed in Table 4 of the Supporting Information. The superposition of the various structures was particularly excellent for the inner nine amino acids (i.e., residues 5−13) with a rmsd of 0.50−0.33 Å, but there was more variation in the terminal residues. The final structure is the average of these 10 final overlapped structures (Figure 7).

To ensure that the final structure was driven by NMR constraints and not by the force field, trial runs were performed without experimental restraints. No convergence was reached for this family of structures (rmsd ≥ 3.0 Å). These large differences clearly indicated that NMR data made a significant contribution in defining the structure of the molecule.

A much more rigorous test of structural accuracy is back-calculation of NOESY spectra based on the final structure. The accuracy of the structures can be judged by comparison with the experimental 2D NOE data. We calculated the theoretical 2D NOE spectra for the restrained structures by complete relaxation matrix analysis using the matrix doubling module of Felix. Figure 4 displays comparisons of representative regions of experimental and back-calculated 150 ms NOESY spectra. Apart from the residual water resonance observed in the experimental NOESY spectrum, the calculated NOESY spectrum yielded very similar cross-peak patterns. The excellent match between back-calculated and experimental spectra pointed out that the final structure not only satisfied the distance restraints but also is consistent with the entire proton relaxation network that generated the time-dependent NOESY spectra.

ELISA Binding Measurements. The affinity of 0.5β for three peptides was measured by a competitive ELISA. One of these peptides represents the sequence of the V3 loop of the HIV-1_{IIIB} strain and contains the GPGR conserved sequence motif at its crown, while the other two peptides have the same sequence, except for thiazolidine derivatives replacing the proline within GPGR. The ELISA plate absorbance is proportional to the fraction of the free antibody. Thus, affinities can be semiquantitatively calculated by a plot of absorbance versus the concentration of competing peptide; the concentration at which absorbance is half-maximal corresponds approximately to K_a. Figure 8 shows the effect of proline replacement on binding of peptides to 0.5β. Replacement of proline with both thiazolidine and 2,2-dimethylthiazolidine does not result in a significant change

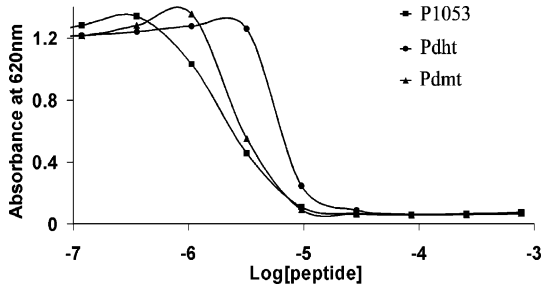

FIGURE 8: Effect of proline replacement on binding of peptides to 0.5β. The antibody was incubated with each peptide at various peptide concentrations, and subsequent inhibition of binding of 0.5β to immobilized peptides was monitored by absorbance of ELISA plate wells.

in competitiveness. The estimated K_a for all three peptides is $\sim 10^6$ M^{-1}. The binding of the Pdht peptide is somewhat weaker.

DISCUSSION

The principal neutralizing determinant of HIV-1 was localized to the third variable V3 loop of the gp120 protein. Using synthetic peptide fragments, Javaherian et al. (*13*) mapped the neutralizing determinant to eight amino acids around a highly conserved Gly-Pro-Gly sequence situated at the tip of the V3 loop and found that peptides of this size were sufficient to elicit neutralizing antibodies. In addition, on the basis of neural network analysis, LaRosa et al. (*18*, *19*) predicted secondary structure for many V3 sequences consisting of two β-strands flanking a type II turn at the Gly-Pro-Gly position (with proline at position $i + 1$) and a short helix in the C-terminal region. More recently, Anglister and co-workers (*27*) elucidated by NMR the structure of a synthetic peptide (P1053) derived from the PND of the V3 loop in interaction with the Fab fragment of an anti-gp120 HIV-1_{IIIB} neutralizing antibody. In contrast to predicted results, they found that the peptide adopted a β-sheet conformation with a type VI β-turn at the RGPG position (with proline at position $i + 2$). This one-residue shift and the difference in the type of turn formed by this peptide were proposed to come from the presence of the Gln and Arg residues prior to the GPGR motif of $V3_{IIIB}$ strain; these residues are absent in other strains, e.g., $V3_{MN}$ peptides (*27*). It was argued that a type VI β-turn could arise from a trans−cis isomerization process occurring at the beginning of the infection. This result was further supported by the high affinity the V3 peptides displayed for immunophilins, which are able to catalyze prolyl trans−cis isomerization (*65*).

Stabilization of the bioactive conformation is one of the most important challenges in therapy. In this context, we decided to stabilize the biologically active conformation of synthetic peptides representing the $V3_{IIIB}$ loop but with the central proline replaced with thiazolidine derivatives, which were shown to be good candidates to mimic a type VI β-turn with the proline-preceding bond in a cis configuration. This peptide was chosen to be similar to that described by the Anglister group (P1035) for direct comparison.

Overall Structure of Pdmt. The structure determination protocol used here was constructed to sample a wide range of conformational space to generate an ensemble of structures that was consistent with the NMR data and that included spin diffusion effects by relaxation matrix calculations (IRMA). The possibility of starting structure dependency in the IRMA calculations was minimized by performing the refinement procedure on two limit initial structures obtained from an extended conformation form and from a β-sheet form and generated by high-temperature simulated annealing. Only those distances that corresponded to nonoverlapped NOE cross-peaks were refined by the IRMA procedure. Other NOE distance and torsion angle restraints were included in the restraint molecular dynamics with larger boundaries appropriate for their experimental errors. A total of 137 distances and 19 dihedral restraints were used for the calculation. The converged structures have low constraint violations, *R*-factors, and rmsd values (Supporting Information). Furthermore, excellent agreement between back-calculated and experimental NOESY spectra was obtained for the resulting final structure (Figures 4). All structure calculations, whether starting from an extended form or a β-sheet conformation, converged to a similar limiting final ensemble of solution structures that are best visualized by the superimposed calculated structures shown in Figure 7.

On the basis of this analysis, our model displayed a clear tendency for the peptide to adopt a β-hairpin conformation, although the NOESY spectra did not show the expected strong interstrand NOEs characteristic of β-sheet formation. This presumably arises from the flexibility of the two strands of the peptide as depicted in Figure 6. However, this result is in good agreement with the relaxation matrix simulation which did not predict such cross-peaks.

Despite the good global homogeneity indicated by rmsd values of 0.93−0.54 Å, the calculated conformers exhibited relatively large variations for terminal parts, because of limited proton−proton distance data available for this peptide. However, well-defined local structure is observed around the peptide loop and particularly from residue 5 to 13, as indicated by rmsd values which were reduced to 0.50−0.33 Å for these amino acids. The β-turn is evident and even better defined since the rmsd decreased further to 0.21−0.13 Å.

Geometry of Pdmt Turn. Type VI β-turns are classified into essentially two subtypes on the basis of the dihedral ϕ and ψ angles of their central $i + 1$ and $i + 2$ residues. In type VIa, the proline ψ dihedral angle value is equal to 0° and the turn is stabilized by intramolecular hydrogen bonding between the carbonyl oxygen of the first residue (i) and the amide hydrogen of the fourth residue ($i + 3$). In type VIb, this stabilizing hydrogen bond is absent and the proline ψ dihedral angle is equal to 160°. Torsion angles of Pdmt were evaluated from the mean lowest-energy structure presented in Figures 7 and 9. For Dmt^{10}, we found the following values: $\omega = 3°$, $\phi = -84°$, and $\psi = 144°$ [which are close to the common values for the type VIb β-turn ($\omega = 0°$, $\phi = -75°$, and $\psi = 160°$ (*66*)]. This result was corroborated by the relatively high value determined for the backbone amide proton temperature coefficient of Gly11 ($|\Delta\delta/\Delta T| > 6$ ppb/K) that is not consistent with the involvement of this proton in an intramolecular hydrogen bond (data not shown).

Free Pdmt versus the Antibody-Bound Structure. Free P1053-like RP135-GKK (*33*) peptides were determined by NMR to be mostly unstructured in solution with the central proline in the trans conformation. However, when bound to the antibody, the peptide adopted a well-defined β-sheet structure adjacent to a central RGPG turn with proline in

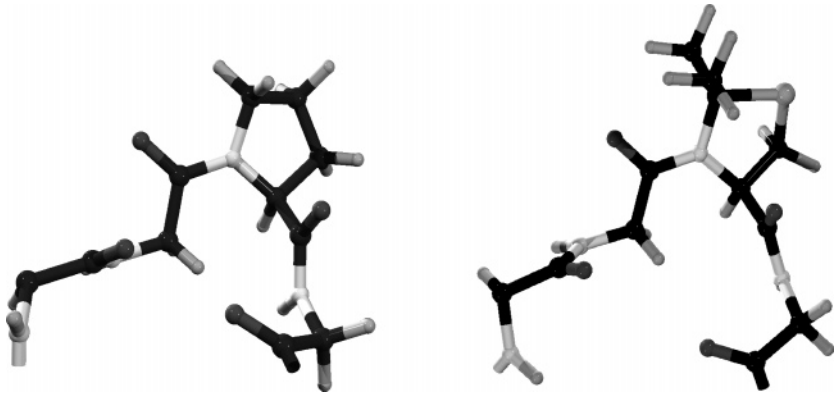

FIGURE 9: Comparison of type VIb with *cis*-proline RGPG β-turn (left) when bound to antibody (from PDB entry 1QNZ) and Pdmt free in water (right).

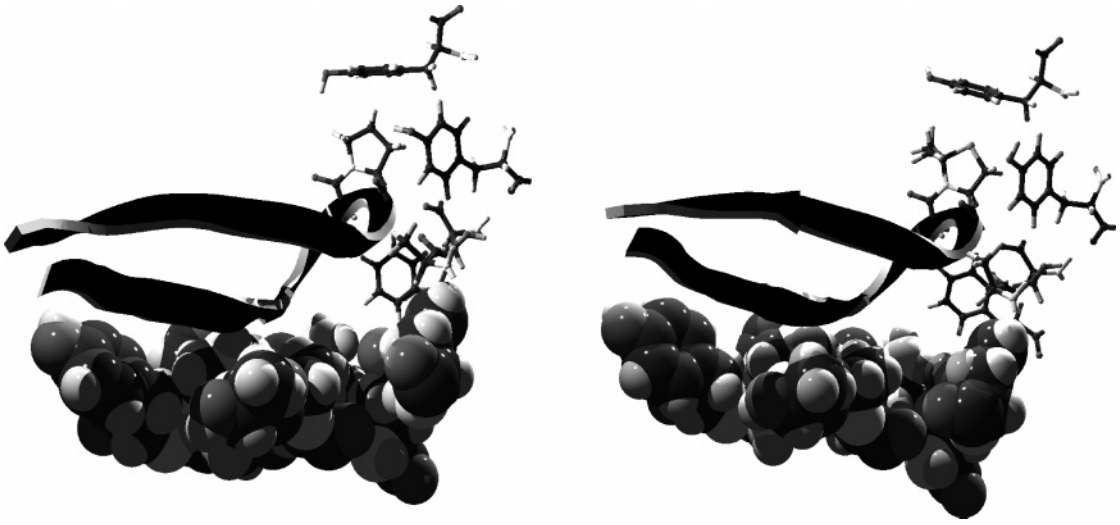

FIGURE 10: Structure of the complex of the 0.5β antibody with the P1053 peptide (left, from PDB entry 1QNZ) and energy-minimized model obtained after replacement of the central proline with Dmt (right). The P1053 peptide is represented by a ribbon with the relevant proline highlighted in stick form. The antibody binding pocket is shown as a space-filling model, and the residues in stick form are those more specifically involved in the interaction with the β-turn.

the cis conformation. The torsion angles found for the bound proline are as follows: $\omega = 0°$, $\phi = -73°$, and $\psi = 127°$ (from PDB entry 1QNZ). These parameters reflect a type VIb β-turn similar to those obtained for Pdmt. As expected, no stabilizing hydrogen bonding is observed in the complex between the carbonyl oxygen of Arg^{8} and the amide hydrogen of Gly^{11}. Furthermore, the latter is involved in intermolecular hydrogen bonding with the carbonyl group of Ser^{95} of the antibody. However, we have noticed that the experimental ψ value is somewhat lower than the classical one (160°), but this discrepancy comes probably from a restriction on the flexibility, due to the hydrogen bond of the amide proton of Gly^{11} to Ser^{95}.

To assess the probable perturbations induced by the two methyl groups present on the Dmt residue when bound to the antibody, we replaced the central proline of the V3−antibody complex with Dmt. The structure obtained after energy minimization shows that the binding cleft of the antibody can accommodate the Dmt residue, quite well. As depicted in Figure 10, no significant steric hindrance occurs from the presence of the methyl groups, making the Dmt residue a good candidate for mimicking type VI β-turns for the V3 peptide.

Peptide Affinities. To estimate the effect of proline replacement on binding of the peptides to the 0.5β antibody, a semiquantitative binding assay based on a competitive ELISA was used. None of the replacements were found to have large effects on binding to the antibody. However, as seen in Figure 8, while Pdmt behaves very much like wild-type P1053 (compare ■ to ▲), the third peptide, Pdht (●), has a lower affinity for the antibody. These results indicate that replacement of proline with 2,2-dimethylthiazolidine has almost no effect and suggest, as also supported by other results, that this derivative successfully mimics the native conformation of the peptide.

In fact, we are convinced that the kinetics of fixation are more favorable for our analogue than for the one with proline because the need for trans−cis isomerization of proline is excluded. However, kinetic constants cannot be obtained from an ELISA test, which rely on thermodynamic parameters.

In conclusion, this work shows that a significant conformational stabilization can be achieved by replacing proline with thiazolidine derivatives properly substituted at C2. In particular, 2,2-dimethylthiazolidine is well suited to mimicking proline in the cis conformation as demonstrated by NMR, molecular modeling, and biological results. It makes only small changes to the overall geometry and does not introduce additional steric clash that could compromise receptor interaction. The Pdmt peptide possesses considerable struc-

tural homology with the type VIb β-turn that the native peptide adopts when bound to the antibody. It also displayed a good propensity to form a β-hairpin conformation similar to that described in the complex. The flexibility of the V3 loop, and particularly the cis conformation, plays an important role in the virus transfection. Therefore, these peptides may be effective immunogens for eliciting anti-HIV antibodies and will be tested as synthetic vaccines in future studies.

The conformational flexibility of peptides in water is one of the principal limitations to the usefulness of synthetic peptides as drugs and immunogens. Thus, stabilization of the structural elements responsible for the specific receptor interaction and for the induction of the biological response is of great pharmacological interest.

ACKNOWLEDGMENT

We thank Dr. D. Boturyn and Dr. J. Becaud for the thiazolidine synthesis and Mrs. Rina Levy for performing the ELISA tests.

SUPPORTING INFORMATION AVAILABLE

Tables of NMR chemical shifts for P1053 and Pdht peptides (Tables 2 and 3) and structural statistics and rmsd values (Table 4). This material is available free of charge via the Internet at http://pubs.acs.org.

REFERENCES

1. Klatzman, D., Champagne, E., Chamaret, S., Gruest, J., Guetard, D., Hercend, T., Gluckman, J. C., and Montagnier, L. (1984) T-Lymphocyte T4 molecule behaves as the receptor for human retrovirus LAV, *Nature 312*, 767−768.
2. Choe, H., Farzan, M., Sun, Y., Sullivan, N., Rollins, B., Ponath, P. D., Wu, L. J., Mackay, C. R., LaRosa, G., Newman, W., Gerard, N., Gerard, C., and Sodroski, J. (1996) The β-Chemokine Receptors CCR3 and CCR5 Facilitate Infection by Primary HIV-1 Isolates, *Cell 85*, 1135−1148.
3. Cocchi, F., DeVico, A. L., Garzino-Demo, A., Cara, A., Gallo, R. C., and Lusso, P. (1996) The V3 domain of the HIV-1 gp120 envelope glycoprotein is critical for chemokine-mediated blockade of infection, *Nat. Med. 2*, 1244−1247.
4. Bazan, H. A., Alkhatib, G., Broder, C. C., and Berger, E. A. (1998) Patterns of CCR5, CXCR4, and CCR3 Usage by Envelope Glycoproteins from Human Immunodeficiency Virus Type 1 Primary Isolates, *J. Virol. 72*, 4485−4491.
5. Berger, E. A., Murphy, P. M., and Farber, J. M. (1999) Chemokine receptors as HIV-1 coreceptors: Roles in viral entry, tropism, and disease, *Annu. Rev. Immunol. 17*, 657−700.
6. Rizzuto, C. D., Wyatt, R., Hernandez-Ramos, N., Sun, Y., Kwong, P. D., Hendrickson, W. A., and Sodroski, J. (1998) A Conserved HIV gp120 Glycoprotein Structure Involved in Chemokine Receptor Binding, *Science 280*, 1949−1953.
7. Starcich, B. R., Hahn, B. H., Shaw, G. M., McNeely, P. D., Modrow, S., Wolf, H., Park, W. P., Josephs, S. F., Gallo, R. C., et al. (1986) Identification and characterization of conserved and variable regions of the envelope gene HTLV-III/LAV, the retrovirus of AIDS, *Cell 45*, 637−648.
8. Leonard, C. K., Spellman, M. W., Riddle, L., Harris, R. J., Thomas, J. N., and Gregory, T. J. (1990) Assignment of intrachain disulfide bonds and characterization of potential glycosylation sites of the type 1 recombinant immunodeficiency virus envelope glycoprotein (gp120) expressed in Chinese hamster ovary cell, *J. Biol. Chem. 265*, 10373−10382.
9. Wu, L., Gerard, N. P., Wyatt, R., Choe, H., Parolin, C., Ruffing, N., Borsetti, A., Cardoso, A. A., Desjardin, E., Newman, W., Gerard, C., and Sodroski, J. (1996) CD4-induced interaction of primary HIV-1 gp120 glycoproteins with the chemokine receptor CCR-5, *Nature 384*, 179−183.
10. Dettin, M., Ferranti, P., Scarinci, C., Picariello, G., and Di Bello, C. (2003) Is the V3 Loop Involved in HIV Binding to CD4? *Biochemistry 42*, 9007−9012.
11. Shioda, T., Levy, J. A., and Cheng-Mayer, C. (1991) Macrophage and T cellline tropisms of HIV-1 are determined by specific regions of the envelope gp120 gene, *Nature 349*, 167−169.
12. Mammano, F., Salvatori, F., Ometto, L., Panozzo, M., Chieco-Bianchi, L., and De Rossi, A. (1995) Relationship between the V3 loop and the phenotypes of human immunodeficiency virus type 1 (HIV-1) isolates from children perinatally infected with HIV-1, *J. Virol. 69*, 82−92.
13. Javaherian, K., Langlois, A. J., McDanal, C., Ross, K. L., Eckler, L. L., Jellis, C. L., Profy, A. T., Rusche, J. R., Bolognesi, D. P., Putney, S. D., and Matthews, T. J. (1989) Principal neutralizing domain of the human immunodeficiency virus type 1 envelope protein, *Proc. Natl. Acad. Sci. U.S.A. 86*, 6768−6772.
14. Ahlers, J. D., Pendleton, C. D., Dunlop, N., Minassian, A., Nara, P. L., and Berzofsky, J. A. (1993) Construction of an HIV-1 peptide vaccine containing a multideterminant helper peptide linked to a V3 loop peptide 18 inducing strong neutralizing antibody responses in mice of multiple MHC haplotypes after two immunizations, *J. Immunol. 150*, 5647−5665.
15. Long, R. D., and Moeller, K. D. (1997) Conformationally Constrained Peptide Mimetics: The Use of a Small Lactam Ring as an HIV-1 Antigen Constraint, *J. Am. Chem. Soc. 119*, 12394−12395.
16. Vu, H. M., Myers, D., de Lorimier, R., Matthews, T. J., Moody, M. A., Heinly, C., Torres, J. V., Haynes, B. F., and Spicer, L. (1999) Nuclear magnetic resonance analysis of solution conformations in C4−V3 hybrid peptides derived from human immunodeficiency virus (HIV) type 1 gp120: Relation to specificity of peptide-induced anti-HIV neutralizing antibodies, *J. Virol. 73*, 746−750.
17. Cabezas, E., Wang, M., Parren, P. W., Stanfield, R. L., and Satterthwait, A. C. (2000) A Structure-Based Approach to a Synthetic Vaccine for HIV-1, *Biochemistry 39*, 14377−14391.
18. LaRosa, G. J., Davide, J. P., Weinhold, K., Waterbury, J. A., Profty, A. T., Lewis, J. A., Langlois, A. J., Dreesman, G. R., Boswell, R. N., Shadduck, P., Holley, L. H., Karplus, M., Bolognesi, D. P., Mathews, T. J., Emini, E. A., and Putney, S. D. (1990) Conserved sequence and structural elements in the HIV-1 principal neutralizing domain, *Science 249*, 932−935.
19. LaRosa, G. J., Davide, J. P., Weinhold, K., Waterbury, J. A., Profty, A. T., Lewis, J. A., Langlois, A. J., Dreesman, G. R., Boswell, R. N., Shadduck, P., Holley, L. H., Karplus, M., Bolognesi, D. P., Mathews, T. J., Emini, E. A., and Putney, S. D. (1991) Conserved sequence and structural elements in the HIV-1 principal neutralizing determinant: Corrections and clarifications, *Science 251*, 811.
20. Ghiara, J. B., Ferguson, D. C., Satterthwait, A. C., Dyson, H. J., and Wilson, I. A. (1997) Structure-based Design of a Constrained Peptide Mimic of the HIV-1 V3 Loop Neutralization Site, *J. Mol. Biol. 266*, 31−39.
21. Wu, G., MacKenzie, R., Durda, P. J., and Tsang, P. (2000) The Binding of a Glycoprotein 120 V3 Loop Peptide to HIV-1 Neutralizing Antibodies, *J. Biol. Chem. 275*, 36645−36652.
22. Stura, E. A., Stanfield, R. L., Fieser, G. G., Silver, S., Roguska, M., Hincapie, L. M., Simmerman, H. K. B., Profy, A. T., and Wilson, I. A. (1992) Crystallization, sequence, and preliminary crystallographic data for an antipeptide Fab 50.1 and peptide complexes with the principal neutralizing determinant of HIV-1 gp120, *Proteins: Struct., Funct., Genet. 14*, 499−508.
23. Rini, J. M., Stanfield, R. L., Stura, E. A., Salinas, P. A., Profy, A. T., and Wilson, I. A. (1993) Crystal structure of a human immunodeficiency virus type 1 neutralizing antibody, 50.1, in complex with its V3 loop peptide antigen, *Proc. Natl. Acad. Sci. U.S.A. 90*, 6325−6329.
24. Stanfield, R., Cabezas, E., Satterthwait, A., Stura, E., Profy, A., and Wilson, I. (1999) Dual conformations for the HIV-1 gp120 V3 loop in complexes with different neutralizing Fabs, *Structure 7*, 131−142.
25. Tsang, P., Mu, X., Wu, G., and Durda, P. J. (1997) NMR Study and Comparison of the Antigenic Properties of a Peptide Recognized by Two HIV-1 Neutralizing Antibodies, *J. Mol. Recognit. 10*, 256−262.
26. Zvi, A., Feigelson, D. J., Hayek, Y., and Anglister, J. (1997) Conformation of the principal neutralizing determinant of human immunodeficiency virus type 1 in complex with an anti-gp120 virus neutralizing antibody studied by two-dimensional nuclear magnetic resonance difference spectroscopy, *Biochemistry 36*, 8619−8627.

27. Tugarinov, V., Zvi, A., Levy, R., and Anglister, J. (1999) A cis proline turn linking two β-hairpin strands in the solution structure of an antibody-bound HIV-1IIIB V3 peptide, *Nat. Struct. Biol. 6*, 331−335.
28. Rosen, O., Chill, J., Sharon, M., Kessler, N., Mester, B., Zolla-Pazner, S., and Anglister, J. (2005) Induced Fit in HIV-Neutralizing Antibody Complexes: Evidence for Alternative Conformations of the gp120 V3 Loop and the Molecular Basis for Broad Neutralization, *Biochemistry 44*, 7250−7258.
29. Weliky, D. P., Bennet, A. E., Zvi, A., Anglister, J., Steinbach, P. J., and Tycko, R. (1999) Solid-state NMR evidence for an antibody-dependent conformation of the V3 loop of HIV-1 gp120, *Nat. Struct. Biol. 6*, 141−145.
30. Balbach, J. J., Yang, J., Weliky, D. P., Steinbach, P. J., Tugarinov, V., Anglister, J., and Tycko, R. (2000) Probing hydrogen bonds in the antibody-bound HIV-1 gp120 V3 loop by solid-state NMR REDOR measurements, *J. Biomol. NMR 16*, 313−327.
31. Vranken, W. F., Budesinsky, M., Martin, J. C., Fant, F., Boulez, K., Gras-Masse, H., and Borremans, F. A. M. (1996) Conformational features of a synthetic cyclic peptide corresponding to the complete V3 loop of the RF HIV-1 strain in water and water/trifluoroethanol solutions, *Eur. J. Biochem. 236*, 100−108.
32. Vranken, W. F., Fant, F., Budesinsky, M., and Borremans, F. A. M. (2001) Conformational model for the consensus V3 loop of the envelope protein gp120 of HIV-1 in a 20% trifluoroethanol/water solution, *Eur. J. Biochem. 268*, 2620−2628.
33. Zvi, A., Hiller, R., and Anglister, J. (1992) Solution conformation of a peptide corresponding to the principal neutralizing determinant of HIV-1IIIB: A two-dimensional NMR study, *Biochemistry 31*, 6972−6979.
34. Catasti, P., Bradbury, E. M., and Gupta, G. (1996) Structure and Polymorphism of HIV-1 Third Variable Loops, *J. Biol. Chem. 271*, 8236−8242.
35. Huang, X., Barchi, J. J., Jr., Lung, F. T., Roller, P. P., Nara, P. L., Muschik, J., and Garrity, R. R. (1997) Glycosylation Affects both the Three-Dimensional Structure and Antibody Binding Properties of the HIV-1IIIB GP120 Peptide RP135, *Biochemistry 36*, 10846−10856.
36. Markert, R. L. M., Ruppach, H., Gehring, S., Dietrich, U., Mierke, D. F., Kock, M., Rubsamen-Waigmann, H., and Griesinger, C. (1996) Secondary structural elements as a basis for antibody recognition in the immunodominant region of human immunodeficiency viruses 1 and 2, *Eur. J. Biochem. 237*, 188−204.
37. Dumy, P., Keller, M., Ryan, D. E., Rohwedder, B., Wöhr, T., and Mutter, M. (1997) Pseudo Prolines as a Molecular Hinge: Reversible Induction of *cis* Amide Bonds into Peptide Backbones, *J. Am. Chem. Soc. 119*, 918−925.
38. Keller, M., Sager, C., Dumy, P., Schutkowski, M., Fischer, G. S., and Mutter, M. (1998) Enhancing the Proline Effect: Pseudo-Prolines for Tailoring *Cis*/*Trans* Isomerization, *J. Am. Chem. Soc. 120*, 2714−2720.
39. Wittelsberger, A., Keller, M., Scarpellino, L., Patiny, L., Acha-Orbea, H., and Mutter, M. (2000) Pseudoprolines: Targeting a cis Conformation in a Mimetic of the gp120 V3 Loop of HIV-1, *Angew. Chem., Int. Ed. 39*, 1111−1115.
40. Johnson, M. E., Lin, Z., Padmanabhan, K., Tulinsky, A., and Kahn, M. (1994) Conformational rearrangements required of the V3 loop of HIV-1 gp120 for proteolytic cleavage and infection, *FEBS Lett. 337*, 4−8.
41. Endrich, M. M., and Gehring, H. (1998) The V3 loop of human immunodeficiency virus type-1 envelope protein is a high-affinity ligand for immunophilins present in human blood, *Eur. J. Biochem. 252*, 441−446.
42. Matsushita, S., Robert Guroff, M., Rusche, J., Koito, A., Hattori, T., Hoshino, H., Javaherian, K., Takatsuki, K., and Putney, S. (1988) Characterization of a human immunodeficiency virus neutralizing monoclonal antibody and mapping of the neutralizing epitope, *J. Virol. 62*, 2107−2114.
43. Wöhr, T., Wahl, F., Nefzi, A., Rohwedder, B., Saxo, T., Sun, X., and Mutter, M. (1996) Pseudo-prolines as a solubilizing, structure-disrupting protection technique in peptide synthesis, *J. Am. Chem. Soc. 118*, 9218−9227.
44. Bayer, E. (1991) Towards the chemical synthesis of proteins, *Angew. Chem., Int. Ed. 30*, 113−129.
45. Chierici, S., Jourdan, M., Figuet, M., and Dumy, P. (2004) A case study of 2,2-dimethylthiazolidine as locked *cis* proline amide bond: Synthesis, NMR and molecular modeling studies of a δ-conotoxin EVIA peptide analogue, *Org. Biomol. Chem. 2*, 2436−2441.
46. Wang, S. S. (1973) p-Alkoxybenzyl alcohol resin and p-alkoxybenzyloxycarbonylhydrazide resin for solid-phase synthesis of protected peptide fragments, *J. Am. Chem. Soc. 95*, 1328−1333.
47. Braunschweiler, L., and Ernst, R. R. (1983) Coherence transfer by isotropic mixing: Application to proton correlation spectroscopy, *J. Magn. Reson. 53*, 521−528.
48. Piantini, U., Sørensen, O. W., and Ernst, R. R. (1982) Multiple quantum filters for elucidating NMR coupling networks, *J. Am. Chem. Soc. 104*, 6800−6801.
49. Willker, W., Leibfritz, D., Kerssebaum, R., and Lohman, J. (1993) Gradient selected E.COSY, *J. Magn. Reson. 102*, 348−350.
50. Griesinger, C., and Ernst, R. R. (1987) Frequency offset effects and their elimination in NMR rotating-frame cross-relaxation spectroscopy, *J. Magn. Reson. 75*, 261−271.
51. Jeener, J., Meier, B. H., Bachmann, P., and Ernst, R. R. (1979) Investigation of exchange processes by two-dimensional NMR spectroscopy, *J. Chem. Phys. 71*, 4546−4553.
52. Hwang, T. L., and Shaka, A. J. (1995) Water suppression that works. Excitation sculpting using arbitrary waveforms and pulsed field gradients, *J. Magn. Reson. 112*, 275−279.
53. Marion, D., and Wüthrich, K. (1983) Application of phase sensitive two-dimensional correlated spectroscopy (COSY) for measurements of ^{1}H-^{1}H spin−spin coupling constants in proteins, *Biochem. Biophys. Res. Commun. 113*, 967−974.
54. States, D. J., Haberkorn, R. A., and Ruben, D. J. (1982) A two-dimensional nuclear Overhauser experiment with pure absorption phase in 4 quadrants, *J. Magn. Reson. 48*, 286−292.
55. Keeler, J., Clowes, R. T., Davis, A. L., and Laue, E. D. (1994) Pulsed-field gradients: Theory and practice, *Methods Enzymol. 239*, 145−207.
56. Bax, A., and Davis, D. G. (1985) MLEV-17 based two-dimensional homonuclear magnetization transfer spectroscopy, *J. Magn. Reson. 65*, 355−360.
57. Shaka, A. J., Lee, C. J., and Pines, A. (1988) Iterative schemes for bilinear operators. Application to spin decoupling, *J. Magn. Reson. 77*, 274−293.
58. Vuister, G. W., and Bax, A. (1993) Quantitative J correlation: A new approach for measuring homonuclear three-bond J(HNHα) coupling constants in ^{15}N-enriched proteins, *J. Am. Chem. Soc. 115*, 7772−7777.
59. Wüthrich, K., Billeter, M., and Braun, W. (1983) Pseudo-structures for the 20 common amino acids for use in studies of protein conformations by measurements of intramolecular proton−proton distance constraints with nuclear magnetic resonance, *J. Mol. Biol. 169*, 949−961
60. Boelens, R., Koning, T. M. G., van der Marel, G. A., van Boom, J. H., and Kaptein, R. (1989) Iterative procedure for structure determination from proton−proton NOEs using a full relaxation matrix approach: Application to a DNA octamer, *J. Magn. Reson. 82*, 290−308.
61. Boelens, R., Koning, T. M. G., and Kaptein, R. (1988) Determination of biomolecular structures from proton−proton NOE's using a relaxation matrix approach, *J. Mol. Struct. 173*, 299−311.
62. Gonzales, C., Rullmann, J. A. C., Bonvin, A. M. J. J., Boelens, R., and Kaptein, R. (1991) Toward an NMR R factor, *J. Magn. Reson. 91*, 659−664.
63. Wüthrich, K. (1986) *NMR of Proteins and Nucleic Acids*, John Wiley and Sons, New York.
64. Wishart, D. S., Bigam, C. G., Holm, A., Hodges, R. S., and Sykes, B. D. (1995) ^{1}H, ^{13}C and ^{15}N random coil NMR chemical shifts of the common amino acids. I. Investigations of nearest-neighbor effects, *J. Biomol. NMR 5*, 67−81.
65. Billich, A., Hammerschmid, F., Peichl, P., Wenger, R., Zenke, G., Quesniaux, V., and Rosenwirth, B. (1995) Mode of action of SDZ NIM 811, a nonimmunosuppressive cyclosporin A analog with activity against human immunodeficiency virus (HIV) type 1: Interference with HIV protein-cyclophilin A interactions, *J. Virol. 69*, 2451−2461.
66. Hutchinson, E. G., and Thornton, J. M. (1994) A revised set of potentials for β-turn formation in proteins, *Protein Sci. 3*, 2207−2216.

BI052615K